

<https://helda.helsinki.fi>

Bicatalytic poly(N-acryloyl glycinamide) microgels

Yang, Dong

2020-06-15

Yang , D , Tenhu , H & Hietala , S 2020 , ' Bicatalytic poly(N-acryloyl glycinamide) microgels
' , European Polymer Journal , vol. 133 , 109760 . <https://doi.org/10.1016/j.eurpolymj.2020.109760>

<http://hdl.handle.net/10138/318493>

<https://doi.org/10.1016/j.eurpolymj.2020.109760>

cc_by_nc_nd

publishedVersion

Downloaded from Helda, University of Helsinki institutional repository.

This is an electronic reprint of the original article.

This reprint may differ from the original in pagination and typographic detail.

Please cite the original version.



Bicatalytic poly(N-acryloyl glycinamide) microgels

Dong Yang, Heikki Tenhu, Sami Hietala*

Department of Chemistry, University of Helsinki, P. O. Box 55, FIN-00014 HU, Finland

ARTICLE INFO

Keywords:

Microgel
Thermosensitive
Enzyme
Silver nanoparticle
Catalysis

ABSTRACT

In both chemo- and biocatalysis the immobilization of catalysts to carriers is often beneficial in terms of catalytic activity and ease of operation. In the present study we encapsulated an enzyme, β -D-glucosidase, inside thermosensitive poly(N-acryloyl glycinamide) microgels by radical polymerization of N-acryloyl glycinamide in the presence of the enzymes. Properties of these hybrid microgels were studied varying the enzyme-monomer ratio and the degree of crosslinking. The enzymatic activities of the microgels were assessed using a model reaction, enzymatic cleavage of p-nitrophenyl- β -D-glucopyranoside under different conditions. The microgel encapsulated enzymes showed enhanced activity at high pH compared to the native enzymes. Once the enzymatic activity of the microgels was ascertained, introduction of silver nanoparticles inside the enzyme carrying microgels was made to develop bicatalytic systems. The bicatalytic microgels were shown to be capable of carrying out a cascade reaction combining enzymatic catalysis and reduction of the reaction product 4-nitrophenol to 4-aminophenol.

1. Introduction

Enzymes are widely utilized in a range of industries due to their ability to catalyze reactions at high specificity under mild conditions [1–3]. Metal nanoparticles (NP) on the other hand fall in the class of chemocatalysts and they are actively studied for heterogeneous catalysis as their large surface to volume ratio enables increased efficiency in many transformations [4,5]. The coupling of enzymatic reactions with metal nanoparticle catalyzed reactions in a tandem fashion can open up new possibilities in organic transformations. However, such catalysis in one-pot often becomes challenging due to inactivation of either or both of the catalysts. As for enzymes, their use is complicated by the intolerance to harsh conditions (e.g. pH or temperature) in their native form. For metal nanoparticle catalysis the small size of NPs together with the high surface energy makes them prone to self-aggregation leading to loss of activity and complicates their separation from the reaction media and concurrent use. For both enzymes and NPs immobilization to suitable nanoscale carriers is a key to their successful application [6,7].

Polymeric carriers are used to encapsulate both enzymes and metal NPs. Among the variety of polymeric structures microgels, nano- or micrometer sized polymer networks capable of forming stable colloidal dispersions in water or other solvents, are used as catalyst carriers [8,9]. Their solvent filled, highly porous structures allow the diffusion of reactants and products in and out of the networked structure

simultaneously stabilizing and allowing the separation of the catalysts after the reaction. Microgel encapsulated enzymes prepared either by *in situ* polymerization [10–14], or by encapsulating the enzymes to pre-formed microgels [15,16] have been reported. In the case of microgel encapsulated metal nanoparticles, the most studied routes are based on the reduction of metal salts, for example gold or silver, inside pre-formed microgels [17–19]. In quest for systems capable of more complex catalytic transformations, cascade or tandem reactions, simultaneous encapsulation of both enzymes and NP catalysts has also been recently demonstrated [20,21].

In addition to simply encapsulating the catalyst to a permeable polymer matrix, the catalytic activity of enzymes or metal nanoparticles can be tuned by employing thermoresponsive polymers. The phase transition of the polymers then provides an additional handle to manipulate the catalytic activity by changes in reactant solubility and permeability and allows also for recovery or reuse of the catalysts. Especially polymers with a lower critical solution temperature (LCST) type of temperature response have been widely used as carriers for enzyme immobilization [22]. However, most of the studied LCST-type thermoresponsive polymers become insoluble below the optimal temperature for enzyme catalysis and the contraction of the polymer may limit the diffusion of the reactants [15,16,23,24]. Upper critical solution temperature (UCST) type polymers are tempting due to their opposite behavior and the fact that they can be recycled by precipitation at low temperatures, but so far they have been used as catalyst carriers

* Corresponding author.

E-mail address: sami.hietala@helsinki.fi (S. Hietala).

<https://doi.org/10.1016/j.eurpolymj.2020.109760>

Received 5 February 2020; Received in revised form 5 May 2020; Accepted 6 May 2020

Available online 11 May 2020

0014-3057/ © 2020 The Authors. Published by Elsevier Ltd. This is an open access article under the CC BY-NC-ND license (<http://creativecommons.org/licenses/by-nc-nd/4.0/>).

with covalently surface immobilized enzymes [25,26].

Here, we present a study of straightforward immobilization of β -D-glucosidase (BG) inside UCST-type thermosensitive poly(N-acryloyl glycinamide) (PNAGA) microgel networks. The BG-PNAGA hybrid microgels are carefully characterized and the effect of encapsulation on the enzymatic catalysis is investigated. Further encapsulation of silver nanoparticles (AgNPs) to the enzyme containing microgels is a simple and efficient way of turning the hybrid microgels into bicatalytic systems.

2. Experimental

2.1. Materials

Glycinamide hydrochloride (Bachem) and acryloyl chloride (Sigma Aldrich) were used as received. N-acryloylglycinamide (NAGA) monomer was prepared as described earlier [19]. N,N'-methylenebis(acrylamide) (BIS, Merck) was recrystallized from methanol. Ammonium persulfate (APS, Merck) was recrystallized from Milli-Q water. N,N,N',N'-tetramethylethylenediamine (TEMED, Merck), β -D-glucosidase from almonds (BG, Sigma Aldrich, nominal molar mass 135000 g/mol), p-nitrophenyl β -D-glucopyranoside (pNPG, Sigma Aldrich) were used as received. Other substances and solvents with the highest purity were used as received. Milli-Q water was used for synthesis and deionised (DI) water for purification. Regenerated cellulose dialysis tubing with a molecular weight cutoff of 12–14 kDa used for polymer purification was from Spectrumlabs.

2.2. Synthesis of enzyme microgels

BG-PNAGA microgels were fabricated with a method adapted from enzyme encapsulated polyacrylamide synthesis reported earlier [10]. The feed ratios for the β -glucosidase, redox initiator APS, catalyst TEMED and stabilizer sucrose were kept constant, while the NAGA monomer and crosslinker BIS concentration were varied. As an example, synthesis of BG-PNAGA6 was done as follows. β -D-glucosidase (9.41 mg, 0.7×10^{-4} mmol), NAGA (53.3 mg, 0.42 mmol), BIS (11.03 mg, 0.072 mmol) and sucrose (250 mg, 0.73 mmol) were first dissolved in 5 mL PBS (50 mM, pH = 6.1) in an 8 mL glass vial followed by purging N_2 for 40 min. The reaction was then initiated by adding TEMED (4.05 mg, 0.035 mmol) immediately after APS (7.96 mg, 0.035 mmol) addition. The reaction mixture was kept at room temperature for 4 h, sampled for conversion determination and extensively dialysed against deionized water followed by lyophilization. The synthesized microgels are shown in Table 1.

2.3. Silver nanoparticle (AgNP) synthesis

The syntheses of the hybrid Ag-BG-PNAGA and Ag-PNAGA microgels was done as previously reported for Ag-PNAGA microgels [19]. Briefly, 14.71 mg of BG-PNAGA6 microgel was dispersed in 5 mL of deionized water. $AgNO_3$ in water (5 mL, 0.32 mg mL^{-1}) was added and the dispersion was kept under stirring purging with N_2 for 2 h before washing out the free Ag^+ by dialysis against deionized water for another 2 h. Fresh aqueous $NaBH_4$ (5 mL, 2.42 mg mL^{-1}) was added

dropwise to microgel dispersion in ice bath to initiate the reduction and reaction continued in ice bath for 4 h before dialysis against deionized water for 24 h. Subsequently, the microgel dispersion was filtered through cotton to remove any possible aggregates and lyophilized.

2.4. Catalysis studies

The enzymatic catalysis was studied by UV following the cleavage of the model compound p-nitrophenyl- β -D-glucopyranoside (pNPG). To monitor the reaction, 3 mL fresh 10 mM pNPG in PBS was added to a standard 10 mm quartz cuvette followed by addition of 50 μ L of enzyme or microgel dispersion under predefined conditions for temperature or pH. The reaction was then followed by monitoring the absorbance change at 405 nm indicating the cleavage of pNPG to 4-nitrophenol, see Supplementary material Figure S1. The apparent reaction rate constant (k_{app}) was calculated from the increment of the absorbance at 405 nm using the pseudo-first order kinetic equation, $\ln(1 - [P]/[C_0]) = -k_{app}t$, where $[P]$ is the concentration of the product, 4-nitrophenol, at time t and $[C_0]$ the concentration of pNPG at the beginning. In order to compare the enzymatic activities of the microgels to the native enzyme, the enzyme content of the microgels was estimated directly from the feed ratios used in the synthesis.

The cascade reaction was tested first allowing the enzymatic cleavage of pNPG (0.89 mM, 3 mL) for a predetermined time using the same protocol as above. Then fresh aqueous $NaBH_4$ (0.5 mL, 12 mg mL^{-1}) was added and the reaction monitored following the absorbance decay at 405 nm indicating the 4-nitrophenol reduction.

2.5. Characterization

The UV-Vis spectra as well as the absorbance changes of pNPG and 4-nitrophenol spectra were recorded on a Jasco V-750 spectrometer equipped with a CTU-100 circulating thermostat unit. 1H NMR spectra of the monomers and polymers were recorded on a 500 MHz Bruker Avance III spectrometer in D_2O . For NMR studies, the sample concentrations were made to 5 mg mL^{-1} in D_2O . Variable temperature intensity changes were analyzed by comparing the areas of the residual HDO solvent signal to the polymer signals. Microcalorimetric measurements of the samples in PBS at pH 6.1 were performed using Malvern Microcal PEAQ-DSC equipped with a measuring cell of 0.13 mL. Heating and cooling scans were made at a heating rate of 60°C/h and sample thermograms obtained by subtracting a baseline recorded for the solvent prior to the measurements. Mean hydrodynamic diameter (D_h) of the microgels (1 mg/mL in PBS at pH 6.1) as a function of temperature were determined using a Malvern Zetasizer Nano ZS (laser wavelength: 633 nm, scattering angle: 173°). Prior the measurements the samples were filtered through 0.45 μ m PVDF filters. TEM measurements were carried out using a Jeol JEM-1400 transmission electron microscope. The microgel samples were placed on a Pioloform coated, glow discharge treated 200 mesh Cu grids and dried at ambient temperature.

Table 1
Enzyme microgel syntheses.

Sample ^a	Type	BG:NAGA [molar ratio]	BIS [mol-% NAGA]	BG [m-%]
PNAGA	reference	0:4200	3	
BG-PNAGA4	high enzyme, low xlink	1:4200	3	19
BG-PNAGA10	low enzyme, low xlink	1:10600	3	8.6
BG-PNAGA6	medium enzyme, high xlink	1:6000	16.7	11.5

^a The sample code refers to excess of NAGA to BG.

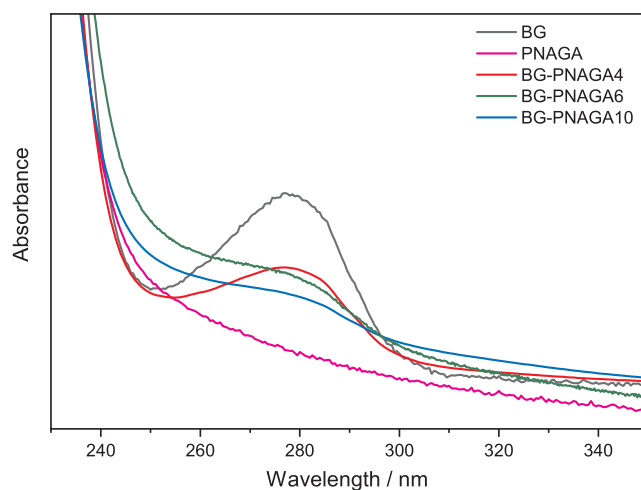


Fig. 1. UV spectra of BG, PNAGA, BG-PNAGA4, BG-PNAGA10, BG-PNAGA6.

3. Results and discussion

3.1. Synthesis of enzyme microgels

Polymerizations of N-acryloyl glycinamide in the presence of β -D-glucosidase were used to prepare BG-PNAGA microgels, Table 1. The syntheses progressed to full conversions during the 4 h reaction time. After reaction the microgels were extensively purified by dialysis in order to remove any free enzyme and low molar mass compounds.

The enzyme encapsulation was first verified by UV-measurements, see Fig. 1. The enzyme containing microgels exhibit the expected BG absorption centered at 260 nm. From the signal intensity it can be seen that the amount of incorporated enzyme is in general in line with the synthesis feed. However, due to the scattering related baseline distortion from the microgel samples, it was deemed unreliable to quantify the enzyme content using UV data. Instead the feed ratios of enzyme and monomer were directly used in quantification of the catalytic activity assuming that all enzyme was incorporated in the microgels.

The enzyme incorporation was further studied by ^1H NMR spectroscopy. The spectra of the BG and BG physically mixed with PNAGA microgel in molar ratio of 1:1000 (mass ratio 1:1) both show clear signals from the enzyme, Fig. 2a. The enzyme containing microgels do not show clear signals arising from the BG. While the BG-PNAGA microgels have only four to ten times smaller amount of incorporated enzyme according to feed ratio compared to the physical mixture, we attribute this behavior to the PNAGA network formation around the enzymes that suppresses the enzyme NMR signals. Furthermore, the NMR spectra shows that the dialysis has removed the low molar mass compounds, especially the sucrose used as stabilizing agent in enzyme encapsulation.

The NMR signal intensities of PNAGA can be used to monitor its UCST-type phase transition behavior as it shows increased signal intensity upon heating. NMR spectra BG-PNAGA6 recorded at different temperatures, Fig. 2b, show that the microgel with encapsulated enzymes retain the thermal response of PNAGA. Compared with pure PNAGA microgel, the incorporation of the enzyme in the network leads to more pronounced polymer signals for BG-PNAGA6 throughout the temperatures studied and the PNAGA phase transition begins at slightly lower temperature. The observations confirm the successful encapsulation of the hydrophilic enzyme inside the gel particles.

Microcalorimetry experiments were performed in order to assess the thermal behavior of the microgels and the enzyme. For PNAGA microgel, the thermogram reveals a broad endothermic transition between 30 °C and 55 °C related to the UCST-type phase transition, Fig. 3. Enthalpic phase transition of PNAGA has earlier been observed for linear, monodisperse PNAGA polymers in water where the transition occurred

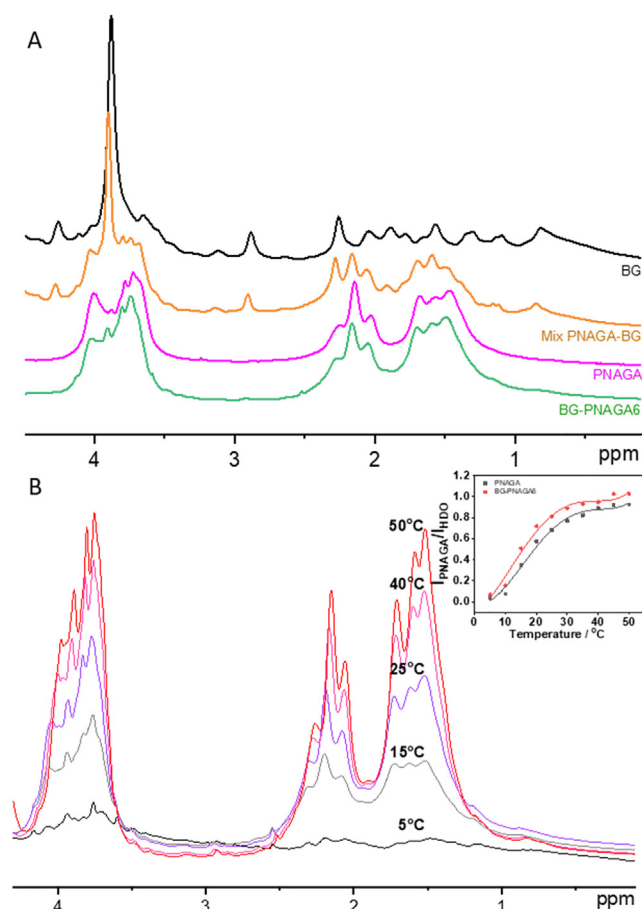


Fig. 2. A) ^1H NMR spectra of BG, a physical mixture of PNAGA and BG, PNAGA and BG-PNAGA6 at 22 °C B) ^1H NMR spectra of BG-PNAGA6 at different temperatures; inset showing the corresponding intensity changes.

at a temperature interval of 5–30 °C [27]. The elevated temperature of the transition in the present case may be related to minute impurities in the NAGA monomer, buffered solvent used or to heterogeneous network structure of the microgels, as the phase transition of PNAGA depends heavily on molar mass and solvent among other factors [27].

β -D-glucosidase on the other hand shows a two-step endothermic transition starting at around 55 °C regardless of concentration, Fig. 3 and S2. Two endothermic maxima are observed, the first at 70 °C and the second at 85 °C. After 85 °C the signal deviates significantly from the baseline. The enthalpy of the transitions, though difficult to quantify accurately due to the BG baseline deviation, is around 300 kJ/mol. According to Tanaka [28] the maxima can be interpreted to originate from unfolding of different domains in the protein and the deviation from the baseline at high temperatures due to aggregation followed by precipitation.

When the PNAGA microgel and BG are physically mixed endothermic transitions of both components are observed, see Fig. 3 and S2. Changing the mixing ratio leads to a change of intensities of the respective endothermic signals. The phase transition temperatures for both components are the same as for the individual components at 1:1 mass mixing ratio, but a slight shift to higher temperature related to BG unfolding is observed when PNAGA is used in excess. For the mixtures the PNAGA phase transition is broadened and the aggregation of BG is suppressed, probably indicating the presence of weak interactions between the enzyme and the polymer. The enthalpy of the BG transition is much lower than that of the free enzyme, of the order of 100 kJ/mol.

The BG-PNAGA microgels also show separate transitions of PNAGA and BG. The PNAGA transition is shifted to lower temperature, which correlates with the variable temperature NMR data. Importantly, the

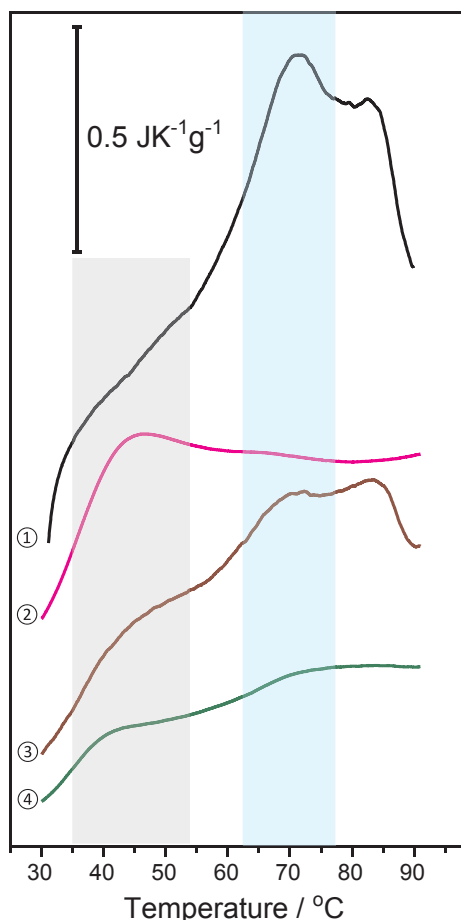


Fig. 3. Concentration normalized thermograms of BG and the microgels 1) BG (1 mg/ml) 2) PNAGA microgel (7 mg/ml) (3) mixture of PNAGA microgel and BG (1 mg/ml, mass ratio = 1:1) 4) BG-PNAGA6 (6 mg/ml). The highlighted areas are to guide the eye.

unfolding transition of BG is shifted to higher temperature, starting at around 65 °C and no baseline distortion takes place at elevated temperatures. The enthalpies of the transitions, although the analyses are complicated by the low signal intensities and the fact that the enzyme content can only be estimated, is lower than that found for the native enzyme. This together with the UV- and NMR-data confirms the incorporation of the enzymes within the PNAGA networks.

DLS analysis of PNAGA and BG-PNAGA microgels shows that the polymerization at room temperature results in microgels with intensity average D_h below 100 nm compared with the size of the native enzyme with D_h around 10 nm, Fig. 4. The increased amount of crosslinker in the feed results in larger sized microgels as observed earlier for polyacrylamide coated nanogels [10]. Upon heating, size increase related to the phase transition of PNAGA can be seen. The size change occurs monotonously for all the studied microgels. When the pure enzyme is studied using the same heating protocol, a clear size increase due to aggregation is observed at around 50 °C. Upon further heating a drastic aggregation takes place, which is not observed in the case of enzyme encapsulated microgels.

3.2. Enzymatic activity

In Fig. 5 the enzymatic activity at different pH for the free and immobilized enzymes are compared by studying the p-nitrophenyl- β -D-glucopyranoside cleavage reaction at 40 °C. The optimal pH for enzymatic activity of BG sourced from almonds is reported to be at pH 5.6 [29] and in the present case the maximum activity is found at pH of 6.1.

For the microgel immobilized BGs the optimal activity shifts to pH 7. At the respective optimal pH of the native enzyme and BG-PNAGA samples their enzymatic activities are generally on the same level. When the activities of the enzymes encapsulated in the microgels are compared, the activity follows the BG:PNAGA ratio used in the synthesis. Here it should be emphasized that the activity calculations of the immobilized enzymes are based on the feed ratio of the enzyme in the microgels. Thus the values do not necessarily represent the actual content of the enzyme leading to underestimation of the enzymatic activity in the case of BG-PNAGA microgels.

When studied at lower pH the enzymatic activity quickly decreases for all the samples. However, notable differences between the free enzyme and BG-PNAGA are observed when at high pH. While the free enzyme loses its enzymatic activity upon increasing pH, the immobilized enzymes retain their activity better. Of the studied enzyme microgels, the highest crosslinker containing BG-PNAGA6 shows enhanced stability up to pH 10, exhibiting still 25% activity compared to the activity at optimal pH.

The enzymatic activity was then assessed at pH 6.1 at different temperatures for the free enzyme and BG-PNAGA6, Fig. 6. The catalytic activity increases with temperature in both samples, but the native enzyme shows more pronounced increase in activity than the microgel immobilized one. Similar temperature trend was reported for covalently immobilized lipase B on UCST-type poly(acrylamide-co-acrylonitrile) particles up to the optimal temperature of 55 °C [26] when compared to the free enzyme. It thus appears that even though the thermosensitive UCST-polymers swell upon heating, the immobilization imposes diffusion limitations compared to the free enzymes. However, compared with the more frequently reported LCST-type polymer-enzyme hybrids, where often a drop in catalytic activity is observed around or above phase transition [15,16,23,24], the situation is improved.

As UCST-type polymers may be suited for a mild recovery by cooling down followed by separation of the reactants, we attempted to recycle the enzyme microgels. However, a significant drop in enzymatic activity was noted at each recycling round. While enzyme inactivation by for example by mechanical stress imposed on the enzymes due to thermally induced swelling/contraction could explain the behavior, we attribute this mainly to the dilute concentration in the assay that leads to incomplete sedimentation of the microgels upon cooling.

In order to make the microgels capable for cascade catalysis, silver nanoparticles (AgNP) were added inside BG-PNAGA6 microgel by reduction of AgNO_3 . TEM images of the pure PNAGA microgels, BG-PNAGA6 and Ag-BG-PNAGA6 are shown in Fig. 7. The microgels without AgNPs can be seen as similar sized objects as observed by DLS. Due to the similar contrast of the enzyme and the PNAGA network, no details of the enzyme encapsulation can be deduced from the TEM images. However, for AgNP containing microgels, similarly as with PNAGA microgels reported earlier [19], multiple AgNPs with size around 5–10 nm are formed inside the microgel particles.

The cascade catalysis was then tested using a protocol where the enzymatic pNPG cleavage was first allowed to proceed producing 4-nitrophenol as the reaction product. The AgNPs further reduce the 4-nitrophenol to 4-aminophenol by addition of NaBH_4 as a cocatalyst. Thus, at a predetermined time NaBH_4 was added and the reaction followed by UV, Fig. 8. First, pure BG and BG-PNAGA6 were studied using the same protocol to rule out the possibility of 4-nitrophenol catalysis without the AgNPs, Fig. 8A. The addition of NaBH_4 abruptly increases the absorption, but β -D-glucosidase and BG-PNAGA6 do not show any further catalytic activity. As a control experiment, NaBH_4 was added to pNPG solution, Figure S3. No abrupt spectral changes are observed without the enzymatically cleaved 4-nitrophenol present.

When catalysis by the AgNP containing Ag-BG-PNAGA6 microgel is studied, Fig. 8B, the abrupt intensity increase takes place upon NaBH_4 addition. However, after a short induction time, Ag-BG-PNAGA6 reduces the 4-nitrophenol completely. To demonstrate that the close

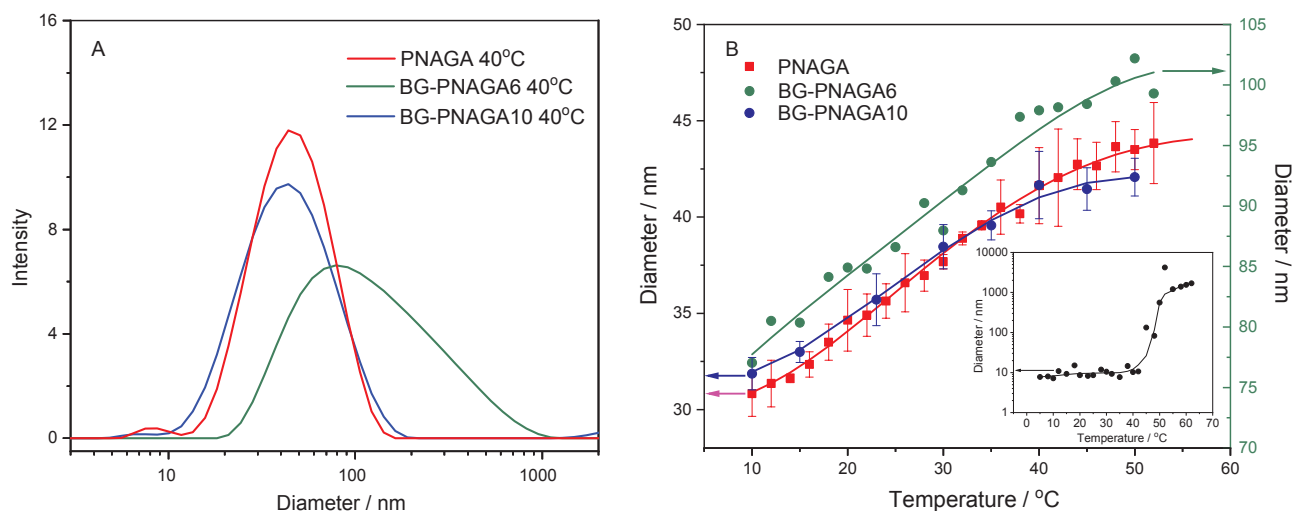


Fig. 4. A) Size distributions of BG, PNAGA, BG-PNAGA6 and BG-PNAGA10 at 40 °C. B) Size variation with temperature upon heating, the inset showing the aggregation of BG.

proximity of the enzyme and chemocatalyst is a necessity for fast reaction kinetics, the same reaction was made using a mixture of BG-PNAGA6 and Ag-PNAGA microgels. As shown in Fig. 8B, when the two catalysts reside in different microgels, the induction time for the AgNP catalyzed reduction of 4-nitrophenol is significantly longer.

To sum up, the results demonstrate that the immobilization of the enzyme into the UCST-type thermosensitive microgels stabilizes them against temperature induced aggregation and increases their activity at high pH. By combining metal nanoparticles into such hybrid microgels cascade catalyses can be realized.

4. Conclusions

β -D-glucosidase was immobilized to crosslinked polymeric microgels of poly(N-acryloylglycinamide), PNAGA, varying the degree of crosslinking and enzyme to polymer ratio. Room temperature radical polymerization of N-acryloylglycinamide in the presence of enzymes resulted in hybrid microgels with hydrodynamic diameter below 100 nm at room temperature. Due to the UCST-type of phase transition of PNAGA, the microgels shrink upon cooling and swell upon heating. During heating, the swelling, as well as enzyme unfolding are

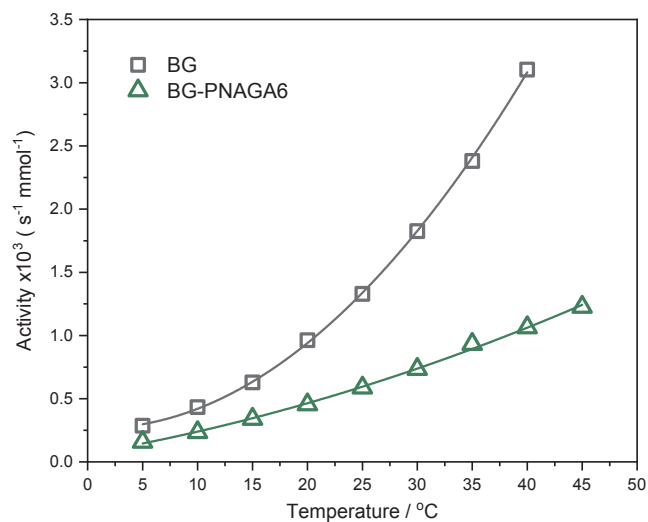


Fig. 6. Apparent kinetic constants of pNGP cleavage at different temperatures at pH 6.1.

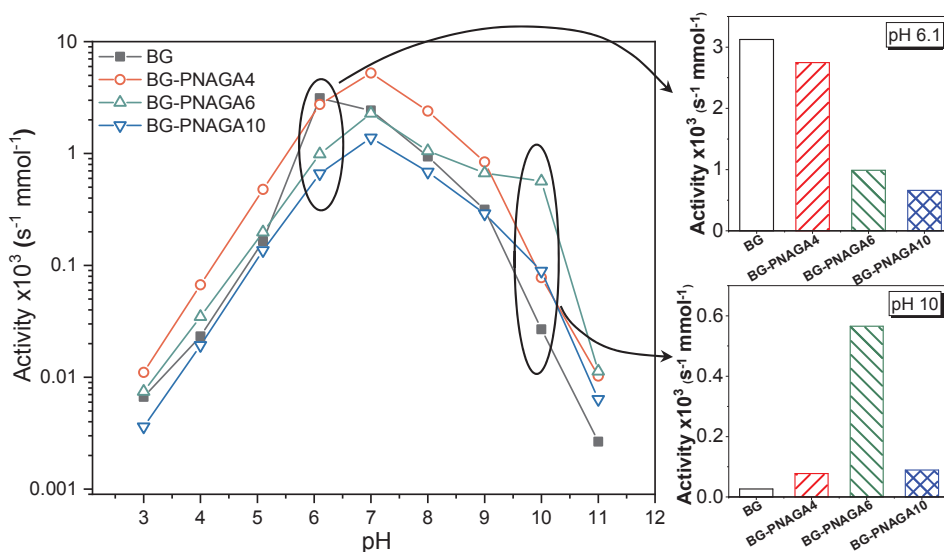


Fig. 5. Enzymatic activity at different pH at 40 °C.

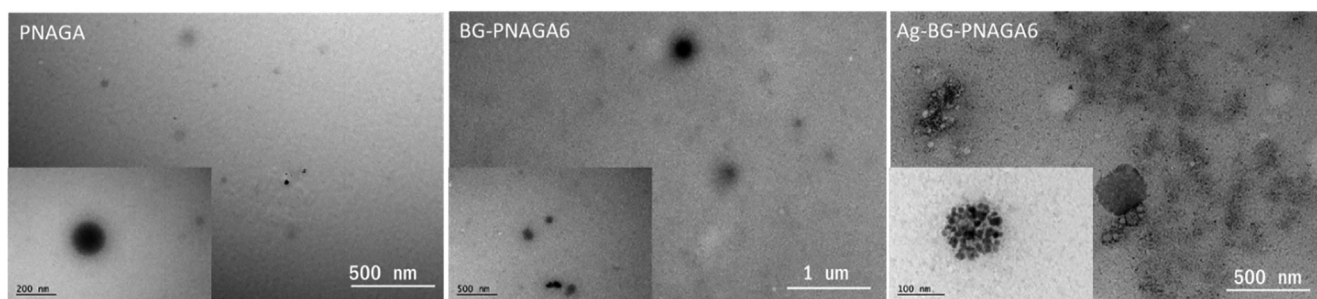


Fig. 7. TEM images of PNAGA, BG-PNAGA6 and Ag-BG-PNAGA6.

accompanied with broad endothermic transitions. The aggregation of BG at elevated temperature was suppressed in the case of the microgel encapsulated enzymes. The enzyme unfolding temperatures increased and the enthalpy of the enzyme unfolding decreased compared to the free enzyme. The enzymatic activity of the enzymes packed in the microgels was assessed under different conditions using a model compound p-nitrophenyl- β -D-glucopyranoside, pNPG. The immobilized enzymes showed comparable activity to the native enzyme at neutral and acidic pH, but retained higher activity at basic pHs. Higher cross-linking degree of the polymeric shell shielded the enzymes and improved their catalytic activity at basic pH. Bicatlytic microgels were produced by adding silver nanoparticles inside the enzyme containing gel particles. The microgels were used in a cascade reaction of enzymatic cleavage of pNPG followed by AgNP catalyzed reduction of the cleavage product 4-nitrophenol to 4-aminophenol.

CRediT authorship contribution statement

Dong Yang: Conceptualization, Methodology, Validation, Formal analysis, Investigation, Writing - review & editing, Visualization.
Heikki Tenhu: Resources, Writing - review & editing, Supervision,

Funding acquisition. **Sami Hietala:** Resources, Writing - review & editing, Supervision, Project administration, Funding acquisition.

Declaration of Competing Interest

The authors declare that they have no known competing financial interests or personal relationships that could have appeared to influence the work reported in this paper.

Acknowledgements

Dong Yang acknowledges the China Scholarship Council PhD grant number 201506950008. We thank the Electron Microscopy Unit of the Institute of Biotechnology, University of Helsinki, for providing laboratory facilities.

Data availability

The raw/processed data required to reproduce these findings cannot be shared at this time due to technical or time limitations.

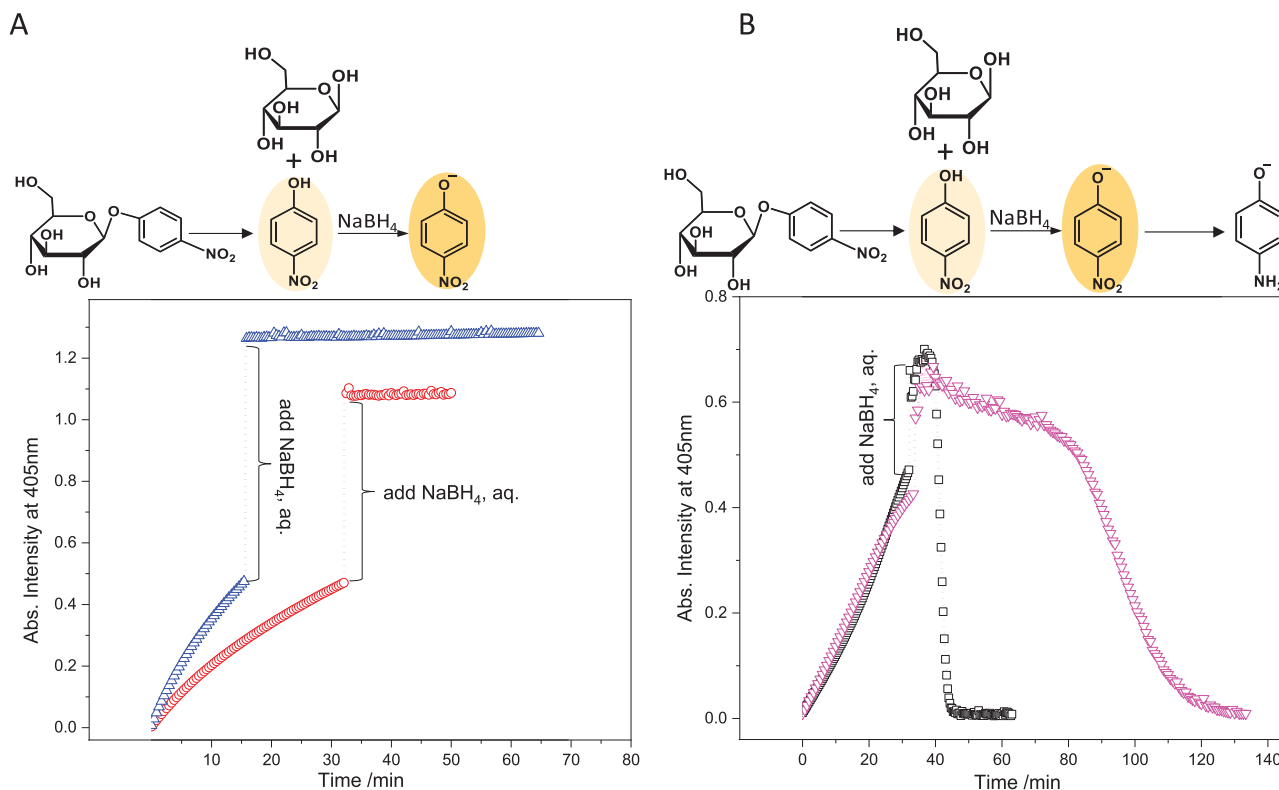


Fig. 8. Cascade catalysis. A) (Δ) BG and (\circ) BG-PNAGA6 B) (\square) Ag-BG-PNAGA6 and (∇) BG-PNAGA6 and Ag-PNAGA mixture.

Appendix A. Supplementary material

Supplementary data to this article can be found online at <https://doi.org/10.1016/j.eurpolymj.2020.109760>.

References

- [1] R.A. Sheldon, S. van Pelt, Enzyme immobilisation in biocatalysis: why, what and how, *Chem. Soc. Rev.* 42 (2013) 6223–6235, <https://doi.org/10.1039/C3CS60075K>.
- [2] J. Zdarta, A.S. Meyer, T. Jesionowski, M. Pinelo, A general overview of support materials for enzyme immobilization: characteristics properties, practical utility, *Catalysts* 8 (2018) 92, <https://doi.org/10.3390/catal8020092>.
- [3] L. Lancaster, W. Abdallah, S. Banta, I. Wheeldon, Engineering enzyme micro-environments for enhanced biocatalysis, *Chem. Soc. Rev.* 47 (2018) 5177–5186, <https://doi.org/10.1039/C8CS00085A>.
- [4] L. Liu, A. Corma, Metal catalysts for heterogeneous catalysis: from single atoms to nanoclusters and nanoparticles, *Chem. Rev.* 118 (2018) 4981–5079, <https://doi.org/10.1021/acs.chemrev.7b00776>.
- [5] T.S. Rodrigues, A.G.M. da Silva, P.H.C. Camargo, Nanocatalysis by noble metal nanoparticles: controlled synthesis for the optimization and understanding of activities, *J. Mater. Chem. A* 7 (2019) 5857–5874, <https://doi.org/10.1039/C9TA00074G>.
- [6] R. Chapman, M.H. Stenzel, All wrapped up: stabilization of enzymes within single enzyme nanoparticles, *J. Am. Chem. Soc.* 141 (2019) 2754–2769, <https://doi.org/10.1021/jacs.8b10338>.
- [7] M. Králik, A. Biffis, Catalysis by metal nanoparticles supported on functional organic polymers, *J. Mol. Catal. Chem.* 177 (2001) 113–138, [https://doi.org/10.1016/S1381-1169\(01\)00313-2](https://doi.org/10.1016/S1381-1169(01)00313-2).
- [8] F.A. Plamper, W. Richtering, Functional microgels and microgel systems, *Acc. Chem. Res.* (2017), <https://doi.org/10.1021/acs.accounts.6b00544>.
- [9] A. Pich, W. Richtering, *Chemical Design of Responsive Microgels*, Springer, 2010.
- [10] A. Beloqui, A.Y. Kobitski, G.U. Nienhaus, G. Delaittre, A simple route to highly active single-enzyme nanogels, *Chem. Sci.* 9 (2018) 1006–1013, <https://doi.org/10.1039/C7SC04438K>.
- [11] S. Reinicke, T. Fischer, J. Bramski, J. Pietruszka, A. Böker, Biocatalytically active microgels by precipitation polymerization of N-isopropyl acrylamide in the presence of an enzyme, *RSC Adv.* 9 (2019) 28377–28386, <https://doi.org/10.1039/C9RA04000E>.
- [12] M. Yan, J. Ge, Z. Liu, P. Ouyang, Encapsulation of single enzyme in nanogel with enhanced biocatalytic activity and stability, *J. Am. Chem. Soc.* 128 (2006) 11008–11009, <https://doi.org/10.1021/ja064126t>.
- [13] A. Beloqui, S. Baur, V. Trouillet, A. Welle, J. Madsen, M. Bastmeyer, G. Delaittre, Single-molecule encapsulation: a straightforward route to highly stable and printable enzymes, *Small* 12 (2016) 1716–1722, <https://doi.org/10.1002/sml.201503405>.
- [14] E. Gau, F. Flecken, A.N. Ksiazkiewicz, A. Pich, Enzymatic synthesis of temperature-responsive poly(N-vinylcaprolactam) microgels with glucose oxidase, *Green Chem.* 20 (2018) 431–439, <https://doi.org/10.1039/C7GC03111D>.
- [15] N. Welsch, A. Wittemann, M. Ballauff, Enhanced activity of enzymes immobilized in thermoresponsive core-shell microgels, *J. Phys. Chem. B* 113 (2009) 16039–16045, <https://doi.org/10.1021/jp907508w>.
- [16] K. Gawlitza, C. Wu, R. Georgieva, D. Wang, M.B. Ansorge-Schumacher, R. von Klitzing, Immobilization of lipase B within micron-sized poly-N-isopropylacrylamide hydrogel particles by solvent exchange, *Phys. Chem. Chem. Phys.* 14 (2012) 9594–9600, <https://doi.org/10.1039/C2CP40624A>.
- [17] Y. Lu, S. Proch, M. Schrunner, M. Drechsler, R. Kempe, M. Ballauff, Thermosensitive core-shell microgel as a “nanoreactor” for catalytic active metal nanoparticles, *J. Mater. Chem.* 19 (2009) 3955–3961, <https://doi.org/10.1039/B822673N>.
- [18] Y. Tang, T. Wu, B. Hu, Q. Yang, L. Liu, B. Yu, Y. Ding, S. Ye, Synthesis of thermo- and pH-responsive Ag nanoparticle-embedded hybrid microgels and their catalytic activity in methylene blue reduction, *Mater. Chem. Phys.* 149–150 (2015) 460–466, <https://doi.org/10.1016/j.matchemphys.2014.10.045>.
- [19] D. Yang, M. Viitasuo, F. Pooch, H. Tenhu, S. Hietala, Poly(N-acryloylglycinamide) microgels as nanocatalyst platform, *Polym. Chem.* 9 (2018) 517–524, <https://doi.org/10.1039/C7PY01950E>.
- [20] Y. Wang, H. Ren, H. Zhao, Expanding the boundary of biocatalysis: design and optimization of in vitro tandem catalytic reactions for biochemical production, *Crit. Rev. Biochem. Mol. Biol.* 53 (2018) 115–129, <https://doi.org/10.1080/10409238.2018.1431201>.
- [21] M. Filice, J.M. Palomo, Cascade reactions catalyzed by bionanostructures, *ACS Catal.* 4 (2014) 1588–1598, <https://doi.org/10.1021/cs401005y>.
- [22] B. Trzebicka, R. Szweda, D. Kosowski, D. Szweda, Ł. Otulakowski, E. Haladjova, A. Dworak, Thermoresponsive polymer-peptide/protein conjugates, *Prog. Polym. Sci.* 68 (2017) 35–76, <https://doi.org/10.1016/j.progpolymsci.2016.12.004>.
- [23] T. Shimoboji, E. Larenas, T. Fowler, A.S. Hoffman, P.S. Stayton, Temperature-induced switching of enzyme activity with smart polymer-enzyme conjugates, *Bioconjug. Chem.* 14 (2003) 517–525, <https://doi.org/10.1021/bc025615v>.
- [24] G.U. Marten, T. Gelbrich, A.M. Schmidt, Hybrid biofunctional nanostructures as stimuli-responsive catalytic systems, *Beilstein J. Org. Chem.* 6 (2010) 922–931, <https://doi.org/10.3762/bjoc.6.98>.
- [25] P.A. Limadinata, A. Li, Z. Li, Temperature-responsive nanobiocatalysts with an upper critical solution temperature for high performance biotransformation and easy catalyst recycling: efficient hydrolysis of cellulose to glucose, *Green Chem.* 17 (2015) 1194–1203, <https://doi.org/10.1039/C4GC01742K>.
- [26] L.-L. Lou, H. Qu, W. Yu, B. Wang, L. Ouyang, S. Liu, W. Zhou, Covalently immobilized lipase on a thermoresponsive polymer with an upper critical solution temperature as an efficient and recyclable asymmetric catalyst in aqueous media, *ChemCatChem* 10 (2018) 1166–1172, <https://doi.org/10.1002/cctc.201701512>.
- [27] J. Seuring, F.M. Bayer, K. Huber, S. Agarwal, Upper critical solution temperature of poly(N-acryloyl glycinamide) in water: a concealed property, *Macromolecules* 45 (2012) 374–384, <https://doi.org/10.1021/ma202059t>.
- [28] A. Tanaka, Differential scanning calorimetric study of the thermal denaturation of almond β -glucosidase, *Agric. Biol. Chem.* 55 (1991) 2773–2776, <https://doi.org/10.1271/bbb1961.55.2773>.
- [29] J. Woodward, A. Wiseman, Fungal and other β -d-glucosidases — their properties and applications, *Enzyme Microb. Technol.* 4 (1982) 73–79, [https://doi.org/10.1016/0141-0229\(82\)90084-9](https://doi.org/10.1016/0141-0229(82)90084-9).